A Permanent Magnets Exciter for Magneto-Rheological Fluid-based Haptic Interfaces

Rocco Rizzo[1,2]

[1]Department of Energy and System Engineering
[2]Research Center "E. Piaggio"
University of Pisa, Italy

***Abstract*—This paper describes an innovative Haptic Interface device based on Magneto-Rheological Fluid (MRF). A system of permanent magnets and coils is designed in order to produce a proper distribution of a magnetic field inside the fluid. This distribution, with its spatial resolution, causes the MRF to assume prescribed shapes and softness profiles that can be directly felt and explored by hand. The device is designed using a 3-D finite-elements code taking into account the B-H functions of the nonlinear materials (MRF, Permanent Magnets, ferromagnetic materials). In order to validate the FEM model, some experimental magnetic measurements are taken on a simplified prototype. Furthermore, the maps of the flux density and those of the shear stress inside the fluid are carefully analyzed. Finally, the interaction between the operator's hand and the MRF is numerically investigated.**

***Index Terms*—Magneto-Rheological Fluids, Electromagnetic devices, Haptic Interfaces.**

I. Introduction

MAGNETO-RHEOLOGICAL Fluids (MRFs) are able to change their rheological behaviour when an external magnetic field is applied [1], [2]. These fluids are synthetic oil-based or water-based suspensions of magnetically polarisable μ-particles. They exhibit a rapid, reversible and tunable transition from a liquid to a near-solid state as a function of the intensity of the magnetic field. This change is manifested by the development of a yield/shear-stress function that monotonically increases with the applied field. This phenomenon is reversible and the fluid can return to its liquid state in a very short time (approx. 10 ms) by removing the magnetic field [3], [4]. Typical MRF applications are in devices used to absorb mechanical shocks or vibrations (e.g. in the automotive or aerospace industry). In previous years, different MRF-based actuators have been developed: MRF dampers both for vehicle or seismic vibrations control, rotary brakes, clutches or valves, and so forth [4]-[12]. The magnetorheological fluid was also used in finishing processes to selectively polish or finish complex-shaped surfaces (optical lens, waveguides, hard disk, ...) [13], [14] .

However, the MRFs have also been used to develop "haptic interfaces" capable of simulating objects in virtual environments. It is possible to produce computer interfaces that allow users to interact with virtual objects by means of force and tactile feedback with these devices. The primary application field for haptic interfaces and displays is in providing a realistic sense of physics to the users immersed in a virtual world.

Conventional haptic devices are based on standard electromechanical actuators that provide forces and torques at the interface with a human operator [15]-[19]. Although such devices (e.g. [20], [21]) are able to provide good replication of "kinaesthetic cues", they cannot address the cutaneous system of receptors. The advantage of using smart fluids in this field comes from the possibility to design and realize a variety of real applications, with "semi-active controls", but without additional mechanical parts [22]-[24]. Alternatively, the effects of rheological fluids can be combined with other actuators such as electromagnetic, pneumatic, or electrochemical actuators so that novel hybrid actuators are produced which can achieve high-power density for relatively low-energy requirements [25]-[28]. Specific design tools can be used in this multidisciplinary context [29]-[32].

Some authors [33]-[37] have already explored the possibility of using rheological fluids in tactile displays, but their attention was focused on the use of Electro-Rheological Fluids (ERFs) [38], [39]. However, a serious drawback associated with the ERFs, is the relatively large "exciting voltage" (typically up to 10 kV) that would prevent the operator to come into direct contact with the fluid.

As for MRFs, at present there are two possible lines of development for haptic interfaces. The first one uses the MRF as an auxiliary material to control forces and torques by means of magnetically controllable devices [40]-[49]. The second line provides a direct contact between the operator and the MRF; the fluid is placed into a plastic box where a hand can be introduced to freely interact with the MR fluid which is properly excited by a magnetic field in order to build figures with a given shape and compliance [50]-[52].

In this paper the latter line is followed and an innovative exciter system is presented. It is made of permanent magnets and coils which are arranged in order to obtain given magnetic field distribution inside the MR fluid.

The paper is organized as follows. Section 2: describes the characteristics of the MR fluid, used to develop haptic interfaces, along with some experimental tests on the fluid itself; Section 3: some prototypes previously developed by the authors are briefly reviewed in order to identify their main drawbacks and potentialities; Section 4: presents the newly

Manuscript received xxxxx; revised yyyy.
Rocco Rizzo - e-mail: rocco.rizzo@dsea.unipi.it;

proposed device and its experimental validation. Finally, a detailed discussion, in terms of flux density and shear stress maps, is given.

II. Characteristics of the used MR Fluid and preliminary tests

Several types of MR fluids have been developed and commercialized in past years. In our applications we used a Magneto-Rheological fluid marked $MRF\ 132LD$, produced by Lord Corporation®, Cary NC, USA [53]. The main characteristics of this fluid, shown in figure 1, can be synthesized as follows:

Magnetic properties: initial relative permeability: $\mu_{r\_initial} \simeq 3.5$; maximum relative permeability: $\mu_{r\_\max} \simeq 7.4$;

Mechanical and rheological properties: maximum yield/shear-stress: $\tau_{\max} \simeq 55 \div 60\ kPa$; response time: $t_{on} \simeq 10\ ms$.

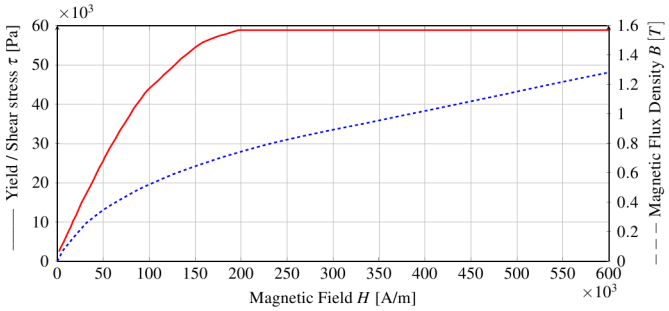

Fig. 1. Magnetic and rheological properties of MRF132LD.

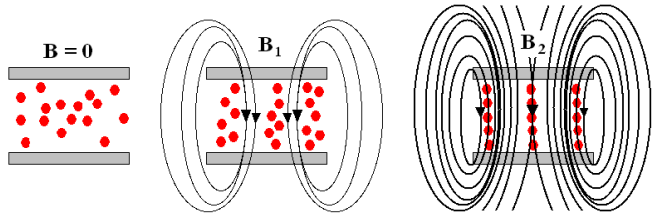

Fig. 2. Schematic view of the operation of a MR fluid ($B_2 > B_1$).

As widely known, it is possible to describe the fluid's behaviour by considering a sample volume of a MRF located in the gap between two plates, as shown in figure 2. In the absence of an applied magnetic field, the fluid freely flows through the gap since the polarisable particles are randomly distributed in the fluid. The application of an external magnetic field produces a controllable yield/shear-stress in the fluid that is almost proportional to the magnitude of the magnetic field itself. In practice, the polarisable particles within the gap, align themselves along the field's force lines (flux lines) creating particle chains that prevent the movement of the fluid particles themselves. In terms of their consistency or softness, controllable fluids appear liquid in the off-state, exhibiting a viscosity ranging from 0.20 to 0.30 $Pa \cdot s$ at 25° C. Figure 1 shows the rheological properties of MRF132LD in steady conditions; as far as the dynamic conditions are concerned, if the magnetic flux density varies from 0 to a given value B, the shear stress value of the fluid follows its characteristic curve with a time delay of a few milliseconds.

From a physical point of view, the MR Fluids exhibit their rheological behaviour operating in "shear", "flow" or "squeeze" mode [4]. Although in many common applications MRFs operate in a single mode, in our application the complete manipulation of a virtual object, simulated inside the MRF volume, is obtained by simultaneously using the fluid's three modes. The electromechanical parameter of interest is the yield/shear-stress $\tau = \tau(B)$ that indicates the transition from a Newtonian-like to a Bingham-like behaviour i.e. from the liquid to the semi-solid state.
The following equations represent a simplified model of the fluids:

$$\begin{cases} \tau < \tau_0(B) & \dot{\gamma} = 0; \\ \tau = \tau_0(B) + \eta\dot{\gamma} & \dot{\gamma} > 0; \end{cases} \tag{1}$$

where $\dot{\gamma}$ is the fluid shear rate, $\tau_0(B)$ is the yield/shear stress as a function of the magnetic flux density, and η is the fluid viscosity with null magnetic field. If an external action produces a shear stress $\tau < \tau_0(B)$, the fluid shear rate is null ($\dot{\gamma} = 0$) and the MRF has a semi-solid behaviour. On the contrary, if $\tau \geq \tau_0(B)$, the fluid shear rate is different from zero ($\dot{\gamma} \neq 0$) and the fluid begins its transition towards a liquid state.

By using the selected fluid's characteristics, we evaluated the possibility to employ MR fluids to mimic the compliance of biological tissues in order to conceive haptic displays for surgical training. In [50] and [54] the MRF's ability to mimic real object softness has been exploited and a set of experiments has been performed. The stress relaxation curves of biological tissues samples and of excited MRF have been compared. The following is a summary of the results.

An MRF specimen has been exposed to an increasing magnetic field applying stepwise strains (strain: 10%, time: 10 s) and so acquiring the relative stress relaxation curve. Since for magnetic flux densities greater than $0.55-0.6$ Tesla, the MRF specimen does not show significant stress relaxation values, the excitation was restricted to $0 \div 0.55\,T$, where differences in the fluid behaviour are more pronounced.

The MRF stress relaxation curves were then compared with those of various biological tissues exposed to the same experimental methodology. Figure 3 shows the latter comparison. It appears that the sample's general behaviour is very similar and it is possible to conclude that with respect to the liver, spleen and brain, a good level of correspondence between the fluid and the tissue's behaviour is attained. Furthermore, as a preliminary psychophysical test, a group of volunteers was asked to use both hands to simultaneously manipulate the biological tissue samples and the MR fluid specimens (duly excited by a magnetic field). Results were very encouraging and in agreement with the initial assumption [54].

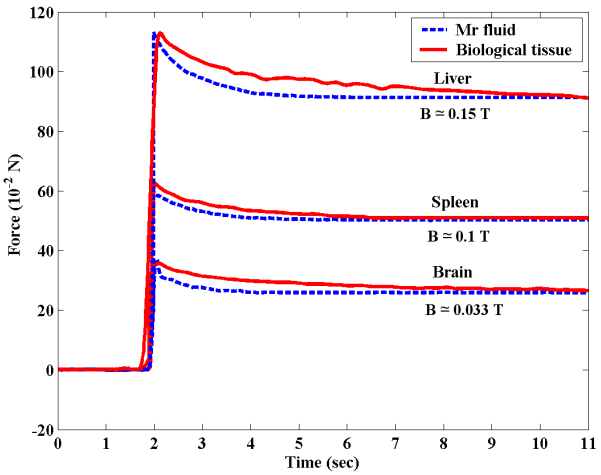

Fig. 3. Comparison between the stress relaxation curves of some biological tissues and the MRF.

III. Previously developed prototypes and their critical issues

A. A brief description

In previous papers [55], [56] the authors presented two innovative Haptic Interface prototypes based on MRFs, in which the user can freely interact with the controlled fluid contained in a box (see figure 4). Unlike other documented kinaesthetic displays, these MRF-based prototypes allow direct hand contact with a compliant object, reproduced in the fluid, involving all the components of the tactile user's perception. The magnetic field in those prototypes has been produced by solenoids properly placed to provide a desired distribution in a given region of the fluid.

In particular, the last operating prototype (Haptic Black Box II: HBB-II), schematic diagram shown in figure 5(a), is composed of a cylindrically shaped plastic box containing the fluid and a series of solenoids and iron pistons.

The solenoids are able to control the position of the iron pistons by moving them in a radial direction in order to reduce or increase the magnetic path's reluctance inside the fluid (lines A-A' and B-B': see figure 5(b)).
The excitation system was designed to focus the magnetic flux into specific regions of the MR fluid, so as to build figures with a given shape and compliance. A properly designed control strategy has allowed us to mimic a wide range of rheological behaviours, within the limits dictated by saturation effects

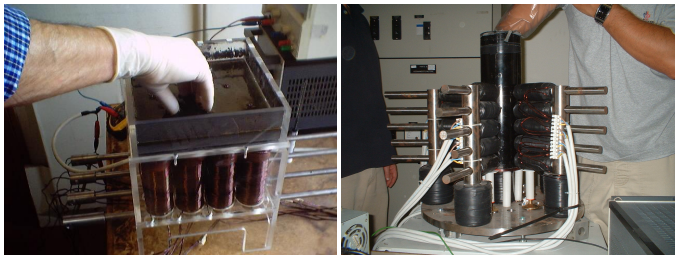

Fig. 4. Pictures of the previously developed prototypes: HBB-I (left) and HBB-II (right).

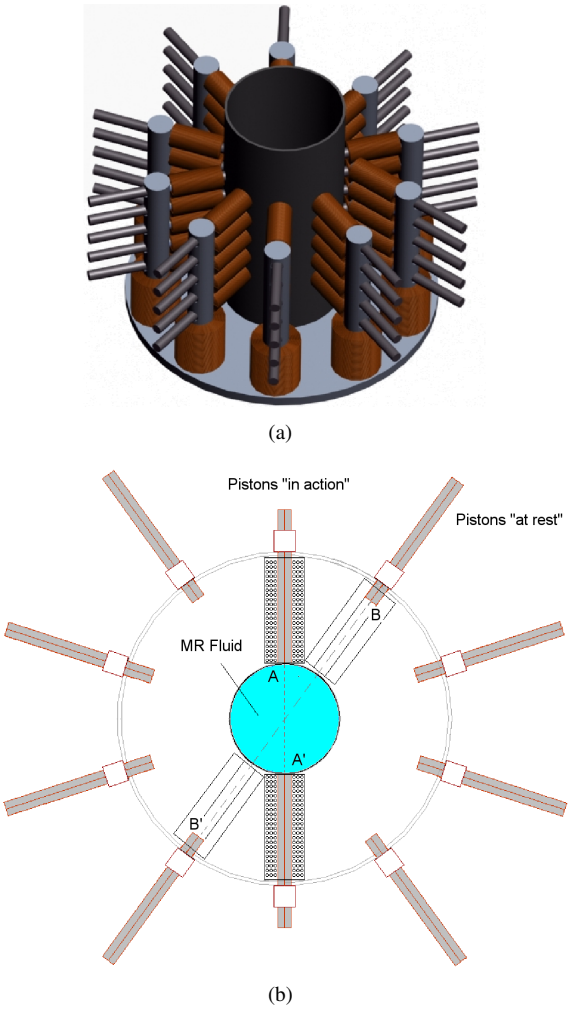

(a)

(b)

Fig. 5. Schematic view of the HBB-II (a), and its operation principle (b).

in the fluid. For example, figure 6 shows one of the many possible configurations that could be obtained with the HBB-II device. In this case, feeding all the pistons on the same surface, the fingers can perceive a little hemisphere on the lateral surface of the box in correspondence with each active mobile piston. However, other complex configurations could be arranged acting both electrically (by varying the value of the current in some of the coils) and mechanically (by moving the pistons along their axial direction) [57]-[59].

B. Critical issues

Although these prototypes seem to work quite well, they have some limitations that must be overcome if a greater set of shapes is to be realized. One of the main problems is related to the system used to excite the MRF in the box. It is widely known that a static magnetic field, governed by Laplace equations, assumes its maxima on the external border and results in a weaker field value in the inner part of the MRF. Furthermore, the number of the pistons and the coils, composing the excitation system, is not high enough to properly "light" the MRF exposed to the magnetic field. It is possible to assess the potential performance of the excitation system, determining the ratio A (in percent) between the surface S_{mrf}

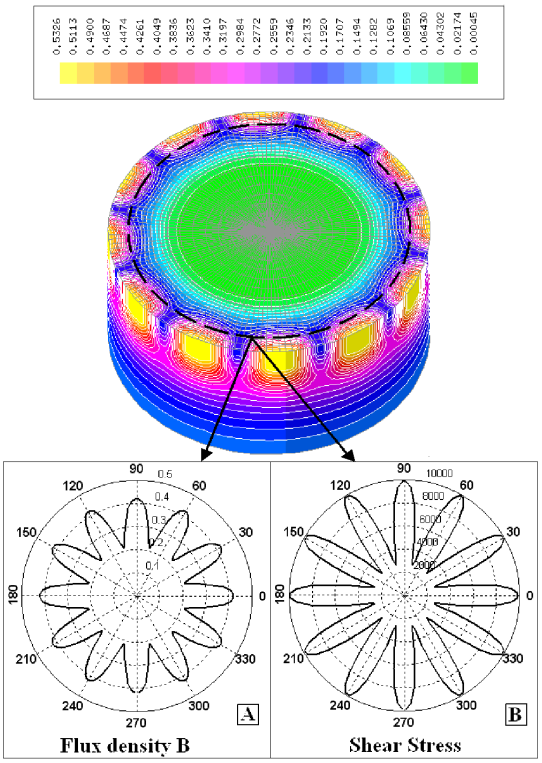

Fig. 6. Map of the flux density in the HBB-II and profile of field (Tesla) and shear stress (Pascal) in a possible excitation configuration.

of the fluid that could be excited by the magnetic field, and the total base surface S_{pist} of the pistons used to really focus the field into the MRF. Taking into account the base and lateral surfaces of the cylindrically shaped plastic box of the HBB-II device (diameter $D = 15\ cm$ and useful height $h = 25\ cm$), the MRF surface is: $S_{mrf} = \pi \cdot (D^2/4 + D \cdot h) \simeq 1355\ cm^2$. The total base surface of the 72 pistons (diameter $d = 2\ cm$), instead, is: $S_{pist} = \pi \cdot d^2/4 \cdot N_{pist} \simeq 226\ cm^2$. This low value is due to the space-consuming coil, positioned around each piston, which does not allow to further increase the pistons number. As a consequence, the value of the ratio is: $A = S_{pist}/S_{mrf} \cdot 100 \simeq 17\%$, revealing a quite low capability of the system to properly excite all the parts of the MRF. However, these critical issues could inhibit the forming of some desired shapes and compliance in the MRF.
In order to overcome the above limitations, a new device will be presented in the next section.

IV. The new proposed device

The improvement of the performance of these innovative MRF-based Haptic Interfaces requires to mainly address the two drawbacks described in the previous section. As for the weakness of the magnetic field in the inner part of the fluid, it can be strengthen by using a flexible box and the permanent magnets as a source of field capable to properly excite such part of the MRF. Moreover, the new device have to strongly increase the ratio A between the surface of the fluid and the total surface of the excitation system. Following these design criteria, a new device, shown in fig. 7, was developed.
The MR fluid fills a flexible plastic balloon (thickness: $\simeq$ 1.5 mm) internally equipped with a latex glove able to handle the fluid. The balloon is placed inside a cubic plastic box with a volume of approx. $3 \times 10^3\ cm^3$, whose base and lateral surfaces compose the exciter system.

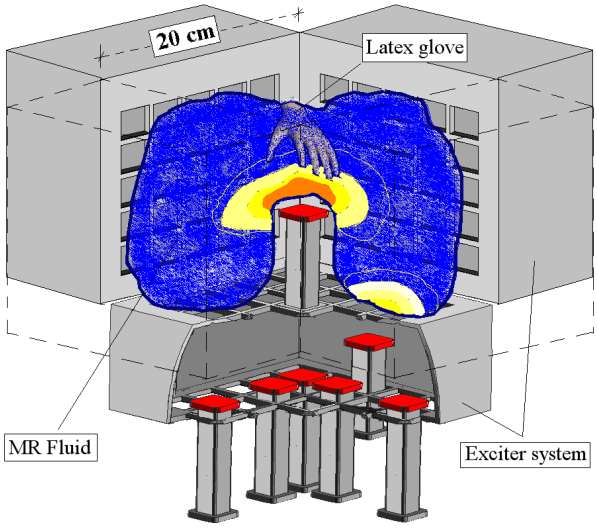

Fig. 7. The schematic view of the new proposed device.

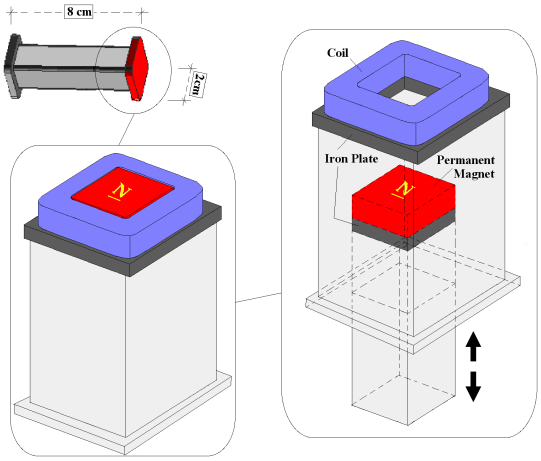

Fig. 8. The exciter system (single unit).

As shown in figure 8, the excitation system is based on an array of exciters, whose single units are composed of small permanent magnets, coils and plastic coaxial columns. A Rare-Earth permanent magnet (PM) is placed on the head of the inner column and on the outer column a double purpose coil is mounted. Its primary purpose is to provide fine control of the field intensity and resolution inside the MRF. Its secondary purpose, as explained later, is to facilitate the separation between the magnet and the fluid after they come into contact. Both the magnet and the coil are glued on an iron substrate in order to focus and control, more efficiently, the magnetic flux density inside the fluid. To achieve the latter control, it is necessary to act both electrically (by varying the value of the current in the coils) and mechanically (by moving the columns, with the PM and the coils, along their axial direction). Each column is then equipped with a linear stepper motor (not shown in figure) that is able to supply the required movement.

TABLE I
Characteristics and dimensions of the exciter system

Part	*Material*	*Physical Characteristics*	*Dimensions [mm]*
PM	NdFeB	$B_r = 1.1\ T$; $H_c = 8.8 \times 10^5\ A/m$;	$15 \times 15 \times 5$
IRON PLATE	AISI 1015	Nonlinear $B_s \simeq 2.05\ T$; $H_s \simeq 0.6 \times 10^5\ A/m$;	$20 \times 20 \times 2$
COIL	Copper wire	$\phi = 0.425\ mm$; Turns: 50; Max Joule Effect: 150 A/mm^2;	Coil section: $\simeq 2 \times 5$;

The characteristics and dimensions of the exciter system are described in table I.

As for the exciter system dimensions, they were chosen on the basis of some previous studies ([50], [60]), in which an analysis about the haptic information necessary to discriminate the softness of objects by touch, and the relation between the contact area and the finger surface, is described. As a consequence, in order to properly "activate" the tactile sensors, the column head surface S_{ch} (PM+coil) was designed to be $4\ cm^2$, that is, as large as an average fingerpad surface (approximately between $3 \div 5\ cm^2$).
The number of the single units composing the excitation system was chosen as a trade-off between an easy accessibility to the fluid, a suitable increase of the ratio A, as defined in the previous section, and an easy realization of the whole system. Then, the excitation system was arranged in 5 set of exciters array (4 for the lateral surfaces and 1 for the base surface, as shown in fig. 7), each of them composed of 25 single units, for a total units number $N_u = 25 \times 5 = 125$.
As for the parameter A, taking into account the dimensions of the new device, its value is: $A = S_{ch} \cdot N_u / S_{mrf} \cdot 100 \simeq 45\%$, where $S_{ch} = 4\ cm^2$, and $S_{mrf} \simeq 1125\ cm^2$ approx. is the surface of the MRF that could be exposed to the magnetic field. The comparison between the previous device (HBB-II) and the new one shows that the value of A in the latter device is increased of about 2.7 times, revealing a better capability to excite the fluid.

A. Operation of the proposed Haptic Interface

The proposed Haptic Interface operates as follows. Let's assume that we want to excite a specific portion of MRF to be felt and explored by hand then, once this region has been chosen, the corresponding columns must be activated moving them along their axial directions. Each column is initially at rest and far enough from the MRF so that the magnetic field does not excite the fluid. During the movement of the column, as the distance between the exciter system (PMs and coils) and the fluid is reduced, the magnetic field inside the MRF increases. The highest values of the magnetic field is obtained when the PM comes into contact with the balloon containing the MRF. However, besides controlling the distance between the magnet and the MRF, the magnetic field could also be modulated by tuning the current in the coil. This combined control allows changes in the MRF's rheology and it obtains different compliance. In this way, many objects of various shapes could be simulated in different zones within the fluid. The new device's ability to address the magnetic field inside the MRF allows the achievement of various quasi-3D virtual objects, showing a higher flexibility than the previously developed devices. Furthermore the exciting system can be pushed inside the MRF as shown in figure 7. This further increases the variety of forms and compliance that can be realized.

B. Numerical Analysis

Since the behaviour of both MRF and permanent magnets is highly nonlinear, an accurate investigation of the proposed system could be performed simply using a numerical analysis. In order to consider the $B - H$ characteristic for nonlinear materials as well as the presence of coils with different feeding conditions, simulation in this paper have been performed using 3D Finite Element (FE) codes MEGA [61] and EFFE [62]. The formulations used in the simulations are briefly described in the appendix section.

The main characteristics of the proposed system appear when analyzing the magnetic flux density distribution produced by the activity of the exciting units in the MRF.

Because of its symmetries, the 3-D FE model could be simplified by modeling only a quarter of the whole structure. The final numerical model contains about 2×10^5 nodes and equations. Figure 9 shows the FE mesh of the device.
The results, in terms of magnetic field inside the fluid and the induced shear-stress, are discussed in section IV-D.

C. Preliminary experimental validation of the device

In order to validate the FEM model, some measurements have been taken of a preliminary simplified prototype, composed of four excitation columns, properly positioned in the space. This validation aims at verifying the device capability to properly excite the fluid, producing a given magnetic field distribution inside specific regions of the MRF. It can be easily obtained comparing the simulated magnetic field with the measured one on the test prototype.

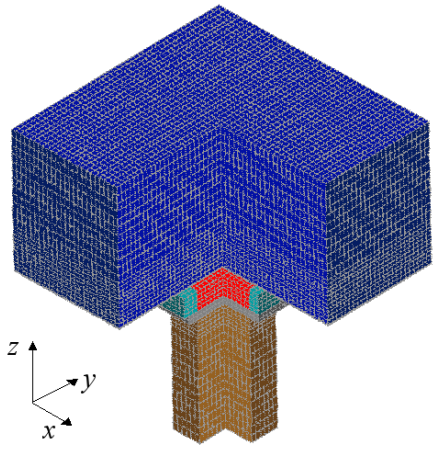

Fig. 9. The 3-D FE model of the system.

The experimental setup, shown in fig. 10, mainly consists of a controllable power supply and a portable Gaussmeter F.W. Bell/4048 equipped with an accurate Hall sensor.
Since it is quite difficult to measure the magnetic field inside the MRF without altering the flux lines, the validation of the model has been carried out referring to the free space. In presence of the fluid, the model validation was performed by means of some indirect measurements taken just outside the balloon filled with MRF.
As an example of the validation procedure in the free space, we used a configuration with only two opposite exciter units. The magnetic field was measured at the points indicated in figure 11 where the distance between the two columns' heads is approximately $5\ cm$. The results are reported in table II, and show a good agreement between the simulated field and the measured one.

Several configurations, not described in this paper for the sake of brevity, were further tested. However, for all of them, the errors between the predicted magnetic field and the measurements were largely below the 10%. As a consequence we can affirm that, from a magnetic point of view, the proposed device is able to properly excite the fluid, producing a given magnetic field distribution inside specific regions of the MR fluid. Furthermore, this preliminary experimental analysis reveals that the developed FEM model can simulate the device operation with acceptable errors.

Fig. 10. Pictures of the excitation preliminary prototype (above) and experimental setup (below).

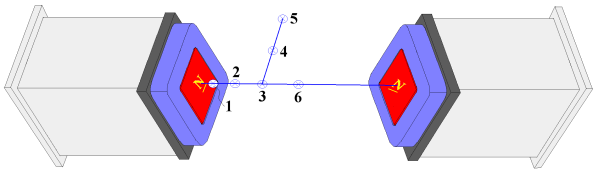

Fig. 11. Measurement points of flux density in the system without the MRF.

TABLE II
Comparison between FEM and experimental measurements

Points of measurements	*Estimated* $\boldsymbol{B}$	*Measured* $\boldsymbol{B}$	$\lvert Error \rvert$
1	$0.307\ T$	$0.3\ T$	$\simeq 2.2\%$
2	$0.194\ T$	$0.18\ T$	$\simeq 7.8\%$
3	$0.103\ T$	$0.11\ T$	$\simeq 6.4\%$
4	$0.0962\ T$	$0.0912\ T$	$\simeq 5.5\%$
5	$0.0493\ T$	$0.0511\ T$	$\simeq 3.6\%$
6	$0.0673\ T$	$0.0618\ T$	$\simeq 8.9\%$

D. Simulation Results and discussion

In order to assess the performance of the device, several simulations were carried out. These aim at obtaining the magnetic flux density distribution B and the induced shear-stress $\tau(B)$ inside the MR fluid for different meaningful excitation configurations. In particular, the quantities B and $\tau(B)$ were calculated in the fluid under the following conditions: a) one exciter unit is "active"; b) two adjacent exciter units are "active"; c) two opposite exciter units are "active". The cases a) and b) were investigated with the PM at a given distance from the fluid and with or without the contribution of the coil to the field B. Furthermore, the configuration a) was analyzed simulating the combined electrical/mechanical control, as described in section IV-A. Finally, a configuration in which an exciter unit reaches an inner part of the fluid was investigated.

Figure 12 shows the flux density in the MRF when only one exciter unit is "active" (configuration a)) with the corresponding coil not fed and with a distance between the PM and the fluid of about $1.5\ mm$ (i.e. the thickness of the balloon).

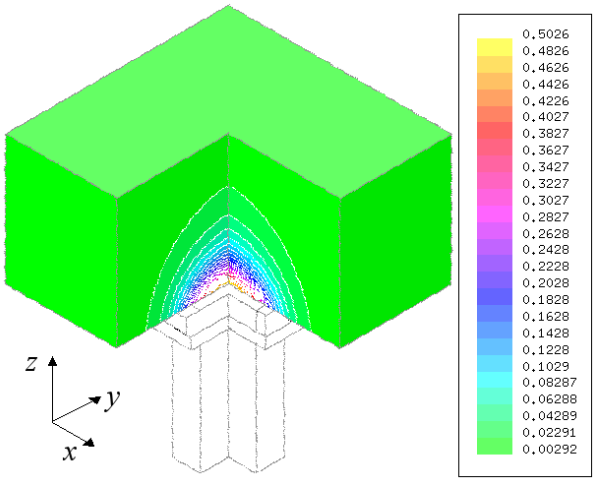

Fig. 12. The flux density (Tesla) in the fluid (configuration a)) when the distance between the PM and the MRF is about $1.5\ mm$.

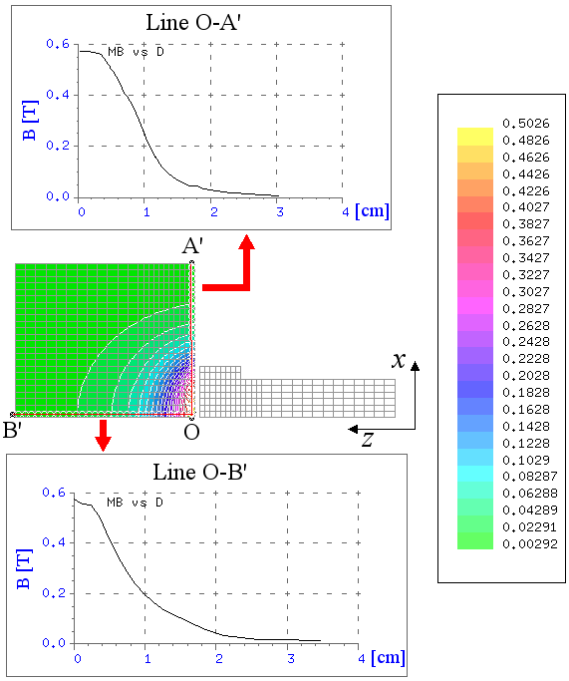

Fig. 13. Map and profiles of the flux density (Tesla) along the lines O-A' and O-B' for the configuration a) (distance: 1.5 mm).

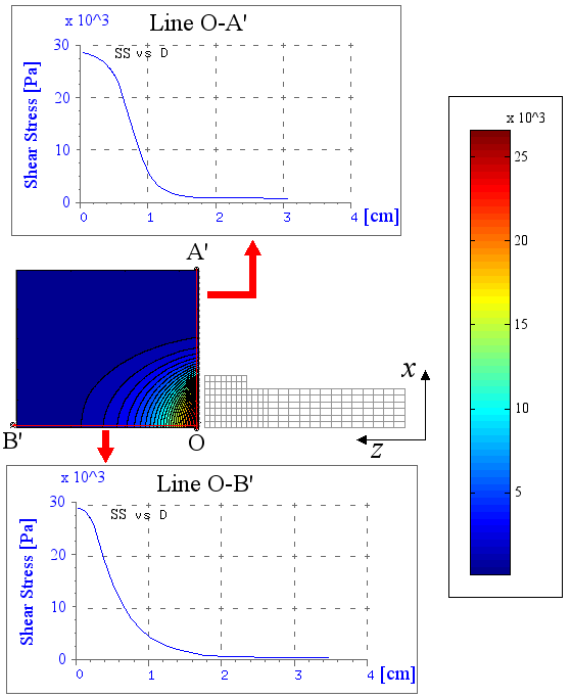

Fig. 14. Map and profiles of the shear stress (Pascal) along the lines O-A' and O-B' for the configuration a) (distance: 1.5 mm).

The flux density map of a cut on the $x-z$ surface at $y=0$ is shown in figure 13. In the same figure the profiles of the flux density along two perpendicular lines are shown: O-A' and O-B', point O being 5 mm inside the MRF.

Here the flux density is high enough ($B \simeq 0.5 \div 0.6\ T$) to result in a high shear-stress and consequently in a semi-solid state of the MRF as shown in figure 14.

An operator who inserts his/her hand into the fluid could perceive one hemisphere positioned at the base or lateral surface of the system. Controlling the PM distance from the MRF and/or the current in the coil, fingers could detect a hemispherical object of different softnesses and consistencies.

Figure 15 shows the flux density map of the $x-y$ surface at a 5 mm distance from the MRF's basis, when two adjacent PMs are "active", with an air gap of 1.5 mm and without current in the coils (configuration b)). The same figure shows the comparison with the configuration a), giving also the flux densities along the same line. However, a suitable current control in the coils allows us to increase/decrease the magnetic field in the area between the two PMs as indicated by the black vertical bar that overlaps the red line (Line B-B'). Figure 16 shows the shear-stress map and its profile, with respect to the field of figure 15.

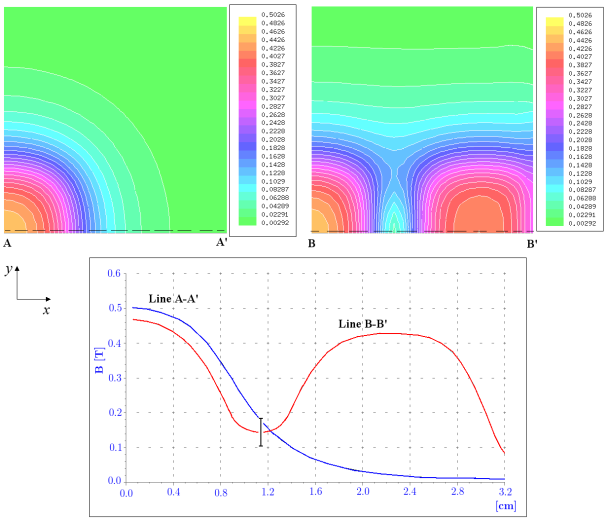

Fig. 15. The flux density maps (Tesla) and profiles along the lines A-A' and B-B' respectively when one or two PMs are activated.

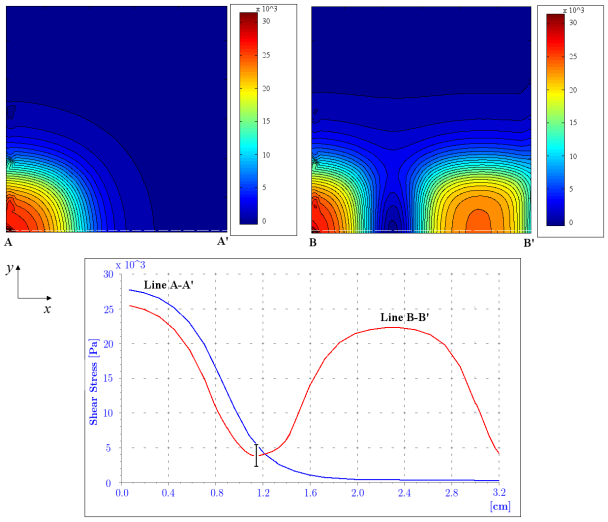

Fig. 16. The shear-stress maps and profiles (Pascal) along the lines A-A' and B-B' respectively when one or two PMs are activated.

An operator who inserts his/her hand into the fluid could perceive two hemispheres (of different softnesses and consistencies) positioned at the base or lateral surface of the system. However, controlling the PMs distance from the MRF and the current in the coils, this configuration could be also perceived as a unique stretched object.

As stated above, the flux density value inside the fluid could be controlled by acting on 1) the distance between the PM and the fluid basis and 2) on the current in the coil placed on the column's head. However the latter modulation could change only approx. $\pm(8-10)\%$ of the value imposed by the magnet acting the field. In figure 17 this combined control, for the configuration a), is simulated showing the flux density profiles along the line A-A' (see figure 15) as a function of the air gap value. The same figure also shows the field variation (around its maximum value) when the corresponding coil is fed by its maximum current (in the same or in the opposite direction to the PM magnetization). Figure 18 shows the shear-stress profile relative to the field shown in the previous figure.

However, this combined control allows a very fine tuning of the viscoelastic parameters in a specific region of the fluid, producing differentials in compliances and plasticity, which can trigger the sensation of touching different objects mimicked by the device.

Figure 19 shows the flux density map in the fluid when two opposite columns are "active" (configuration c)). In this case fingers could perceive a little parallelepiped with softness and consistence related to the applied magnetic field.

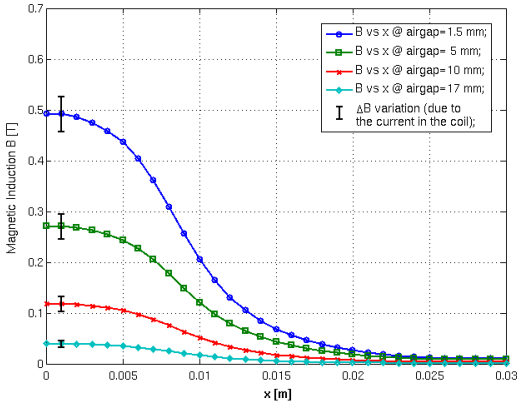

Fig. 17. The flux density profile along the lines A-A' (see figure 15) as a function of the airgap value.

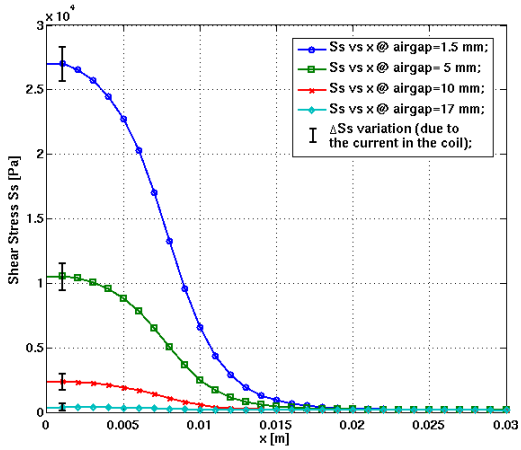

Fig. 18. The shear stress profile along the lines A-A' (see figure 16) as a function of the airgap value.

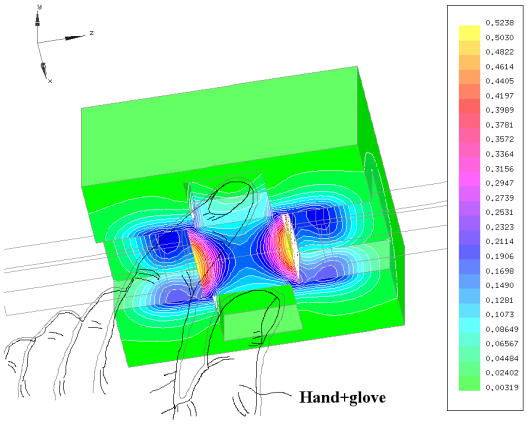

Fig. 19. The flux density map of (Tesla) in the fluid when two opposite PMs are "active".

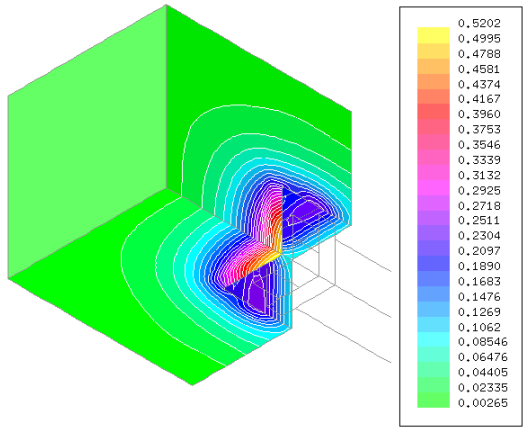

Fig. 20. The flux density map (Tesla) in the fluid when the PM enters' into the fluid for a depth of approx. 8 mm.

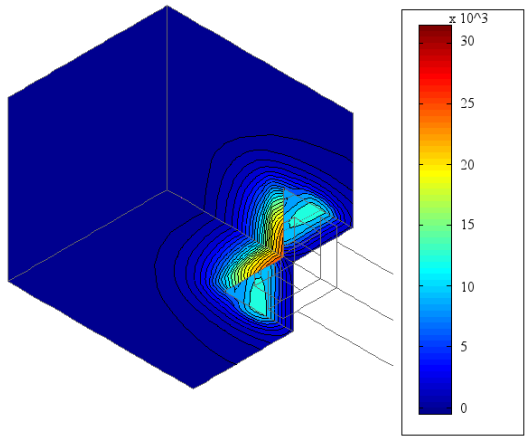

Fig. 21. The shear stress map (Pascal) in the fluid when the PM enters' into the fluid for a depth of approx. 8 mm.

Figure 20 shows the flux density 3D map when a PM column enters' into the fluid for a depth of approx. $8\ mm$. As figure 21 shows, in this case the excited fluid surrounds the column's head allowing the operator to perceive a little sphere of a given softness. Some preliminary tests have proved that the excited fluid volume is thick enough to prevent the contact between the fingers and the column's head. However, by properly activating several "exciting" units, many other field configurations could be obtained. Therefore it is possible to mimic different objects of desired shapes, softnesses and compliance. In particular, figure 22 shows some of these shapes, obtained inside the MRF by the contemporary activation of four or more exciter units: a hollow square-shaped (a), a L-shaped (b), a cross-shaped object (c), an arrow-shaped (d), a single big hemispherical cap (e), a double big hemispherical cap (f), and so forth.

Furthermore, by activating the exciter units in a predefined sequence, a dynamic behaviour of the MR fluid can be obtained. Therefore, it is possible 1) to "move" the shapes along a given path inside the fluid, 2) to dynamically change the profile of a shape surface, or 3) to create a traveling wave of MRF, with a given speed dictated by the actuators response time.

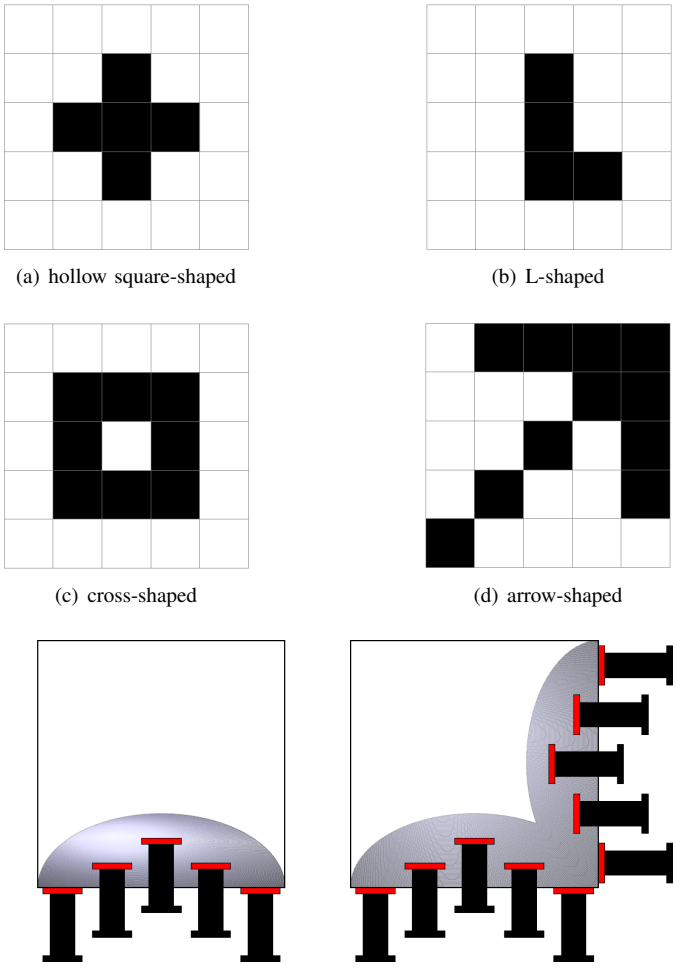

(a) hollow square-shaped (b) L-shaped

(c) cross-shaped (d) arrow-shaped

(e) single hemispherical cap (f) double hemispherical cap

Fig. 22. Examples of possible shapes that can be obtained inside the MRF.

Fig. 23. Picture of the hollow square-shaped object, obtained inside the MR fluid.

Finally, in order to assess the capability of the device to reproduce some of the described shapes inside the fluid, a rough test was developed. An open rigid plastic box was filled with the fluid and then its basis was excited by using the simplified prototype described in section IV-C. Figure 23 shows a picture of a test example in which the hollow square-shaped object is clearly distinguishable.

E. The force of attraction between PM and MRF

The MRF magnetic permeability varies in a range of approx. 3 and 7, depending on the operating point. As a consequence, the interacting PM-MRF develops an "attractive" magnetic force that must be counterbalanced to separate the magnet from the fluid. This is achieved using the coil situated on the outer column's head.

Figure 24 shows the values of the force of attraction between PM and MRF when the PM is touching the balloon, obtained by means the FE model. The dashed red line refers to the case where there is no current in the coil. The value of force is approx. $3.5\ N$. When the two parts must be separated, the coil positioned around the magnet is feed with a $50\ A$ current pulse for approx. $150\ ms$. During this time the force of attraction falls down to approx. $0.65\ N$ value while an auxiliary solenoid actuator (not described here) can provide a synchronized force

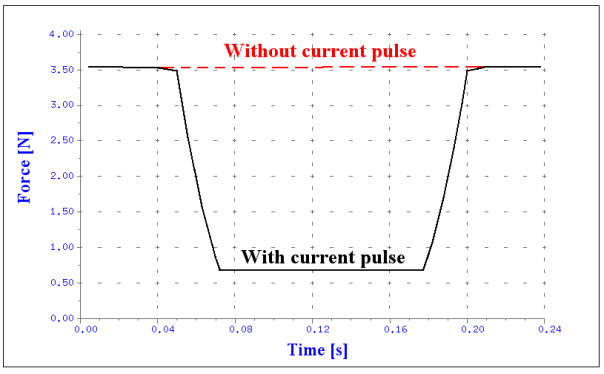

Fig. 24. Profile of the force of attraction between PM and MRF with or without a feeding current pulse of about $50\ A/150\ ms$ (the PM is touching the balloon).

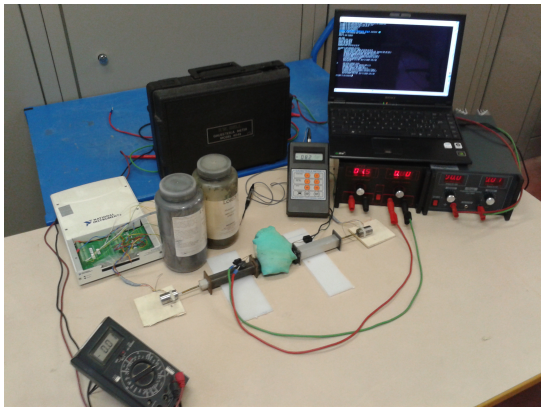

Fig. 25. Experimental setup used to evaluate the force of attraction between the PM and MRF.

pulse capable of separating the PM from the fluid [63], [64]. These forces have also been evaluated by using an integral numerical formulation described in [65] - [69], and the differences with respect the FEM values are within 5%.
The current pulse intensity in the coil has been chosen in order to avoid wire damages due to the overheating. The heating caused by the Joule effect is kept below the maximum allowed temperature to ensure insulation between the wires. Furthermore the magnetic field produced by the current pulse in the Rare-Earth material is approx. $2\times10^5\ A/m$ that is quite below the "coercivity" of the NdFeB ($H_c \simeq 8.8\times10^5\ A/m$) allowing a safe separation procedure.
Figure 25 shows an experimental setup used to evaluate the force between the PM and MRF. The force value, measured without a current pulse in the coil, is approx. $3.2\ N$ with approx. 8.5% error between the simulated and the measured force. Anyhow, when the coil is fed with a ($50\ A/150\ ms$) current pulse the measured force is approx. $0.6\ N$ with an error of about 7.7%.

F. Interaction between operator's fingers and the MRF

As described in the above sections, the proposed device is equipped with a latex glove allowing an operator to feel and explore the excited fluid. The hand (wearing the glove) has a magnetic permeability typical of free space ($\mu_r \simeq 1$), while the MRF is a nonlinear material with a permeability ranging from 3.5 to 7.5, depending on the magnetic flux density value. When the fingers are inserted into the fluid, the force lines' paths are altered with respect to their distribution previous to the hand insertion. Obviously the device expected behaviour must be independent from the hand insertion; i.e. once chosen portion of an MRF is energize the hand's presence in the proximities of the magnetic flux must not interfere with the distribution of the flux itself. Two measures could be suggested in order to reduce the perturbation produced by hand insertion. The first one is based on the use of an array of magnetic field sensors to be positioned in the fluid and employed for a feedback control system.

A second solution is based on the choice of a proper glove material [70]. If the hand+glove system is able to exhibit an average magnetic reluctance similar to that of the MRF, then the interaction between the operator's hand and the fluid would produce a reduced perturbation of the magnetic flux density in the surrounding MRF. Using the theory of the magnetic flux tubes, the domain occupied by the hand (magnetic permeability μ_0) and the glove material (thickness of about $1\ mm$ and unknown magnetic permeability μ_x) has been subdivided into several flux tubes. The whole domain reluctance is obtained by means of the widely known magnetic circuit laws. Then, equating this reluctance with that of the same region, supposedly filled with MRF (with $\mu_r = 5.0$, value corresponding to B in the range 0.3-0.5 T), a quadratic equation is obtained in terms of the unknown permeability of the glove material. The solutions of this equation are: $\mu_{r_{x_1}} = 10.5$ and $\mu_{r_{x_2}} = -0.24$, where the obvious choice is the first one.

A numerical simulation has been performed in order to verify the chosen solution. Figure 26 shows the maps of the flux density distribution inside the fluid when a hand, wearing the designed glove, feels a specific volume of excited MRF. Figure 27 shows the the flux density profiles along the line A-A' (positioned at $8\ mm$ from the PM head) for three different configurations. The blue profile represents the field when the whole volume only contains MRF (no interaction). The red profile refers to the condition where an operator explores the fluid wearing a standard glove ($\mu_{glove} \simeq 1$). Finally, the green profile represents the flux density when the inserted hand wears the designed glove (magnetic permeability $\mu_{glove} = 10$). The figure clearly shows that the flux density distribution is appreciably modified by the insertion of the hand (wearing a conventional glove, i.e. the one with $\mu_r = 1.0$) with respect to the distribution registered when only MRF is present. The differences are approx. $20-22\%$. Alternatively, when using the proposed glove, the flux density B in the evaluated region (the one where the MRF has a semisolid behaviour) has a value only slightly perturbed and this demonstrates the quality of the proposed solution.

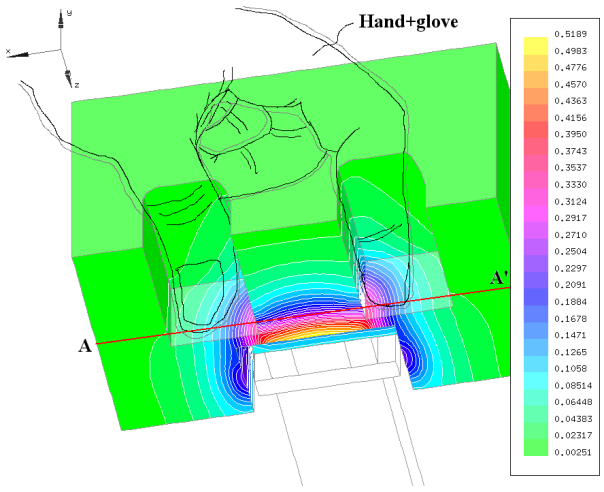

Fig. 26. Interaction between an operator's hand and the excited MRF (flux density in Tesla and $\mu_{glove} = 10$).

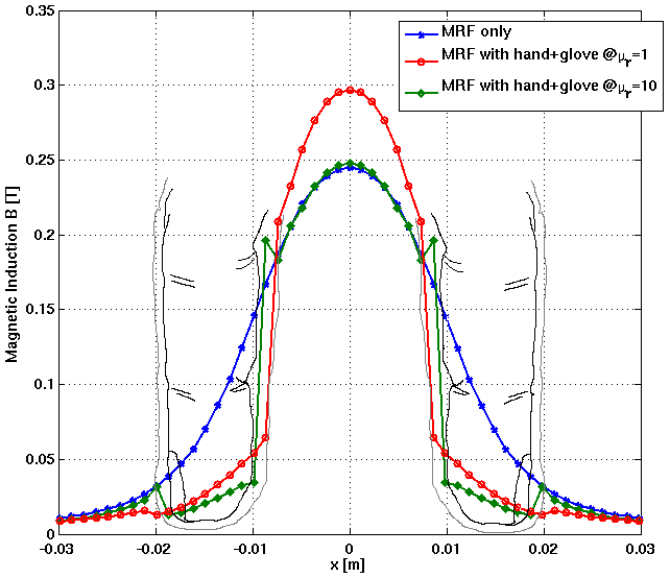

Fig. 27. Profile of the flux density as a function of the magnetic permeability of the different materials along the line A-A' of the previous figure.

V. Conclusion and Future Work

In this paper a new system for Magneto-Rheological Fluids excitation for Haptic Interfaces has been described. The system is based on an array of NdFeB permanent magnets and coils and it has been simulated by means of a 3-D Finite Elements code. The non-linearity of the materials as well as the feeding condition of the coils have been taken into account. The obtained results have shown good performance in terms of field intensity and its spatial resolution inside fluid.

Moreover, the problem of the interaction between the operator's hand and the MRF has been analyzed and a simple solution has been proposed. Preliminary tests have confirmed an improvement in terms of softness and/or shape reconstruction with respect to the previous prototypes.

The work is now progressing towards the actual realization of the full-scale prototype and towards the psychophysical tests needed to verify the capability of the device to mimic virtual objects of different shapes, softnesses and compliances. In these tests some volunteers will be asked to interact with the MR fluid (at different excitation grades) and required to describe the perceived sensations. Several experiments should be developed in which the subjects should recognize, for example, the position, shape and orientation of simple figures inside the MRF, or to assess the compliance between real and mimicked objects.

Appendix

Field formulation in the used FEM software

For 3D non-conducting regions, which contain no source current, the formulation is expressed in terms of total magnetic scalar potential ψ:

$$\mathbf{H} = -\nabla\psi \tag{2}$$

$$\nabla \cdot (\mu \nabla \psi) = 0; \tag{3}$$

In the region containing known source currents (e.g. coils), the magnetic field could be split into two parts: the source field $\mathbf{H}_s$ and the gradient of a "reduced scalar potential" ϕ. Using this formulation for regions containing known source of currents, it is possible to write:

$$\mathbf{H} = -\nabla\phi + \mathbf{H}_s \tag{4}$$

and consequently:

$$-\nabla \cdot (\mu \nabla \phi) + \nabla \cdot (\mu \mathbf{H}_s) = 0 \tag{5}$$

where μ is the non-linear function of the B-H characteristics and $\mathbf{H}_s$ is the field created by the source current calculated using Biot-Savart law:

$$\mathbf{H}_s = \frac{1}{4\pi} \int J \times \nabla \left(\frac{1}{r}\right) dV \tag{6}$$

If the region contains permanent magnets the equation is:

$$\nabla \cdot (\mu \nabla \psi) = \nabla \cdot \mathbf{B}_{rem}. \tag{7}$$

Finally, the different regions are coupled by the FE code using the usual boundary conditions which express the continuity of the flux density's normal component B_n, and of the magnetic field strength's tangential components H_t. This allows us to use the best formulation in each region of the system.

References

[1] J.D. Carlson, "The Promise of Controllable Fluids", *Proc. of Actuator 94* (H. Borgmann and K. Lenz, Eds.), AXON Technologies Consult GmbH, pp. 266-270, 1994.

[2] J.D. Carlson, D.N. Catanzarite and K.A. St Clair,"Commercial Magneto-Rheological Fluid Device", *Proceedings 5th Int. Conf. on ER Fluids, MR Suspensions and Associated Technology*, W. Bullough, Ed., World Scientific, Singapore, pp.20-28, 1996.

[3] C.W. Macosko, "Rheology: Principles, Measurements, and Applications", 1994, New York: VCH Publishers, Inc..

[4] W. I. Kordonsky, "Elements and devices based on magnetorheological effect", *J. Intell. Mater. Syst. Struct.*, vol. 4, no. 1, pp. 65-69, 1993.

[5] W.I. Kordonsky, "Magnetorheological Effect as a Base of New Devices and Technologies", *Journal of Magnetism and Magnetic Materials*, 1993, Vol. 122, No. 1-3, pp. 395-398.

[6] A. Savost'yanov, "Effects of Magnetomechanical Relaxation in a Magnetorheological Suspension", *Magnetohydrodynamics*, 1992, Vol. 28, No. 1, pp. 42-47.

[7] Z.P. Shulman, W.I. Kordonsky, and Zaitsgendler, "Structure, Physical Properties and Dynamics of Magnetorheological Suspensions", In *Int. Journal of Multiphase Flow*, 1986, Vol. 12, No. 6, pp. 935-955.

[8] A.M. Kabakov, A.I. Pabat, "Controlled Magnetorheological Shock Absorbers", *Magnetohydrodynamics*, 1990, Vol. 26, No. 2, pp. 222-227.

[9] General Motors Corporation, *http://www.cadillac.com/cadillacjsp/models/seville/ridecontrol.jsp*

[10] Delphi Automotive, *http://www.delphiauto.com/pdf/chassispdfs/magneride.pdf*, 2002.

[11] R. Rizzo, A. Musolino, F. Bucchi, P. Forte, F. Frendo, "A fail-safe magnetorheological clutch excited by permanent magnets. Magnetic FEM analysis and experimental validation", *IOP-Smart Mater. Struct.*, vol. pp. 1-28, 2013.

[12] F. Bucchi, P. Forte, F. Frendo, A. Musolino, R. Rizzo, "A fail-safe magnetorheological clutch excited by permanent magnets. Design and prototype testing", *IOP-Smart Mater. Struct.*, pp. 1-20, 2013.

[13] Sang-No Lee, Joon-Ik Lee, Yong-Jun Kim, Jong-Gwan Yook, "Low-Loss Thin Film Microstrip Lines and Filters Based on Magnetorheological Finishing.", In *IEEE Transactions on Components and Packaging Technologies*, Vol. 30, Issue 4, pp. 849-854, 2007.

[14] A.B. Shorey, S.D. Jacobs, W.I. Kordonski, R.F. Gans, "Experiments and Observations Regarding the Mechanisms of Glass Removal in Magnetorheological Finishing.", In *Applied Optics*, Vol. 40, Issue 1, pp. 20-33, 2001.

[15] Alaimo, S.M.C., Pollini, L., Magazz, A., Bresciani, J.P., Robuffo Giordano, P., Innocenti, M., Blthoff, H.H., "Preliminary evaluation of a haptic aiding concept for remotely piloted vehicles". In EuroHaptics 2010 Conference, July 2010.

[16] Lam, T.M., Boschloo, H.W., Mulder, M., Van Paassen, M.M., "Artificial force field for haptic feedback in UAV teleoperation". IEEE Transactions on Systems, Man and Cybernetics, Part A. Vol. 39, Issue 6, 2009.

[17] Alaimo, S.M.C., Pollini, L., Bresciani, J.P., Blthoff, H.H., "A comparison of direct and indirect haptic aiding for remotely piloted vehicles", *19th IEEE International Symposium in Robot and Human Interactive Communication*, IEEE Ro-Man 2010.

[18] Alaimo, S.M.C., L. Pollini, J.P. Bresciani, H.H. Blthoff, "Evaluation of Direct and Indirect Haptic Aiding in an Obstacle Avoidance Task for Tele-Operated Systems", *IFAC World Congress 2011*, Milan Italy.

[19] Alaimo, S.M.C., L. Pollini, J.P. Bresciani, H.H. Blthoff, "Experimental Comparison of Direct and Indirect Haptic Aids in Support of Obstacle Avoidance for Remotely Piloted Vehicles", *Journal of Mechanics Engineering and Automation (JMEA)*, vol. 2, no. 10, pp. 628-637, 2012.

[20] M. de Pascale, G. de Pascale, D. Prattichizzo, and F. Barbagli, "A new method for haptic gpu rendering of deformable objects.", In *Proc. of EuroHaptics 2004*, Munich, Germany, 5-7 June 2004.

[21] A. Barbagli, A. Frisoli, K. Salisbury; M. Bergamasco, "Simulating human fingers: a soft finger proxy model and algorithm", In *Proc. 12th Int. Symposium on Haptic Interfaces for Virtual Environment and Teleoperator Systems*, HAPTICS 2004, pp. 9-17.

[22] Y. Grasselli, G. Bossis, and E. Lemaire, "Field-Induced Structure in Magnetorheological Suspensions", *Progress in Colloid & Polymer Science*, 1993,Vol. 93, pp. 175-177.

[23] E. Lemaire, Y. Grasselli, and G. Bossis, "Field Induced Structure in Magneto and Electro-Rheological Fluids" *Journal de Physique*, Vol. 2, No. 3, pp. 359-369.

[24] G. Bossis and E. Lemaire, "Yield Stresses in Magnetic Suspensions", *Journal of Rheology*, vol. 35, no. 7, pp. 1345-1354, 1991.

[25] Y. Guozhi, M. Guang and F. Tong, "The characteristics of electrorheological fluid and its application for vibration control", *Journal of Machine Vibration*, vol. 4, pp. 232-240, 1995.

[26] A.M. Kabakov and A. I. Pabat, "Development and Investigation of Control Systems of Magnetorheological Damper", *Soviet Electrical Engineering*, vol. 61, no. 4, p. 55, 1990.

[27] V.A. Fedorov , "Features of Experimental Research into the Characteristics of Magnetorheological and Electrorheological Shock Absorbers on Special Test Stands", In *Magnetohydrodynamics*, vol. 28, no. 1, pp. 96-98, 1992.

[28] W. Kordonsky, O. Ashour, and C.A. Rogers, "Magnetorheological Fluids: Materials, Characterization, and Devices". *Journal of Intelligent Material Systems and Structures*, 1996. 7: p. 123-130.

[29] R. Bassani, E. Ciulli, F. Di Puccio, A. Musolino, "Study of Conic Permanent Magnet Bearings", *MECCANICA*, vol. 36, no. 6, pp. 745-754, 2001.

[30] S. Barmada, A. Musolino, R. Rizzo, M. Tucci, M., "Multi-resolution based sensitivity analysis of complex non-linear circuits", *IET Circuits, Devices and Systems*, vol. 6, no. 3, pp. 176-186, 2012.

[31] R. Albanese, M. Canali, A. Musolino, M. Raugi, G. Rubinacci, S. Stangherlin, "Analysis of a Transient Nonlinear 3-D Eddy Current Problem with Differential and Integral Methods", *IEEE Trans. Mag.*, vol. 32, no. 3, pp. 776-779, 1996.

[32] M. Toni, et. al, "Modelling of electromechanical devices by GPU accelerated integral formulation", *Int. J. of Num. Modelling: Electron. Networks, Devices and Fields*, 2012, Published online in Wiley Online Library (wileyonlinelibrary.com). DOI:10.1002/jnm.1860, p. 1-21.

[33] H. Böse, G.J. Monkman, H. Freimuth, H. Ermert, M. Baumann, S. Egersdörfer, and O. T. Bruhns, "ER Fluid Based Haptic System for Virtual Reality", *8th Int. Conference on New Actuators & 2nd Int. Exhibition on Smart Actuators and Drive Systems* , pp.351-354, 10-12 June 2002, Bremen, Germany.

[34] P.M. Taylor, A. Hosseini-Sianaki, C.J. Varley, "Surface Feedback for Virtual Environment Systems Using Electrorheological Fluids", *Int. Journal of Modern Physics B*, Vol. 10, No. 23 & 24, 1996, pp. 3011-3018.

[35] P.M. Taylor, D.M. Pollet, A. Hosseini-Sianaki, C. J. Varley, "Advances in an Electrorheological Fluid Based Tactile Array", *Displays*, Vol. 18, pp.135-141, 1998.

[36] G. Burdea, and P. Coiffet, *Virtual Reality Technology*, John Wiley and Sons: New York, NY, 1994.

[37] G.J. Monkman, "An Electrorheological Tactile Display", in *Presence (Journal of Teleoperators and Virtual Environments)*, Vol.1, issue 2, pp. 219-228, MIT Press, July 1992.

[38] Y. Bar-Cohen, C. Mavroidis, M. Bouzit, B. Dolgin, D. L. Harm, G. E. Kopchok, R. White, "Virtual reality robotic telesurgery simulations using MEMICA haptic system", In *Proc. of SPIE's 8th Annual International Symposium on Smart Structures and Materials*, 5-8 March, Newport, CA. Paper No. 4329-47 SPIE, 2001.

[39] J. Fricke, and H. Baehring, "Design of a tactile graphic I/O tablet and its integration into a personal computer system for blind users", *Electronic proceedings of the 1994 EASI High Resolution Tactile Graphics Conference*.

[40] J.D. Carlson, "Portable hand and wrist rehabilitation device", US Patent No.: 6117093.

[41] Blake, J.; Gurocak, H.B.; "Haptic Glove With MR Brakes for Virtual Reality", *IEEE/ASME Transactions on Mechatronics*, Vol. 14, no. 5, pp. 606-615, 2009.

[42] Kikuchi, S.; Hamamoto, K.; "HAMA device - Haptic display for Immersive Virtual Environments", *International Symposium on Communications and Information Technologies, 2008*, pp. 453-458, 2008.

[43] Cassar, D.J.; Saliba, M.A.; "A force feedback glove based on Magnetorheological Fluid: Preliminary design issues", *15th IEEE Mediterranean Electrotechnical Conference, 2008*, pp. 618-623, 2010.

[44] Winter, S.H.; Bouzit, M.; "Use of Magnetorheological Fluid in a Force Feedback Glove", *IEEE Transactions on Neural Systems and Rehabilitation Engineering*, Vol. 15, no. 1, pp. 2-8, 2007.

[45] Savioz, G.; Ruchet, V.; Perriard, Y.; "Study of a miniature magnetorheological fluid actuator for haptic devices", *IEEE/ASME International Conference on Advanced Intelligent Mechatronics, 2010*, pp. 1197-1202, 2010.

[46] Tae-Heon Yang; Hyuk-Jun Kwon; Lee, S.S.; Jinung An; Jeong-Hoi Koo; Sang-Youn Kim; Dong-Soo Kwon; "Conceptual design of mniniature tunable stiffness display using MR fluids", *Solid-State Sensors, Actuators and Microsystems Conference, 2009*, pp. 897-899, 2009.

[47] Heintz, B.; Fauteux, P.; Letourneau, D.; Michaud, F.; Lauria, M.; "Using a Dual Differential Rheological Actuator as a high-performance haptic interface", *IEEE/RSJ International Conference on Intelligent Robots and Systems, 2010*, pp. 2519-2520, 2010.

[48] Senkal, D.; Gurocak, H.; "Compact MR-brake with serpentine flux path for haptics applications", *EuroHaptics conference, 2009 and Symposium on Haptic Interfaces for Virtual Environment and Teleoperator Systems. World Haptics 2009.*, pp. 91-96, 2009.

[49] B Liu, WH Li1, P B Kosasih and X Z Zhang, "Development of an MR-brake-based haptic device",*IOP - Smart Materials and Structures*, 15 (2006) 1960-1966

[50] E.P. Scilingo, A. Bicchi, A. De Rossi, A. Scotto, "A magnetorheological fluid as a haptic display to replicate perceived compliance of biological tissues", *1st Annual International IEEE-EMBS Special Topic Conference on Microtechnologies in Medicine & Biology*, Lyon, France, October 12-14, 2000.

[51] E. P. Scilingo, N. Sgambelluri, D. De Rossi, and A. Bicchi, "Haptic Displays Based on Magnetorheological Fluids: Design, Realization and Psychophysical Validation", *In Proc. 11th Symp. on Haptic Interfaces for Virtual Environment and Teleoperator Systems*, pages 10-15, 2003.

[52] A. Bicchi, E. P. Scilingo, N. Sgambelluri, D. De Rossi, "Haptic Interfaces based on magnetorheological fluids", *Proc. 2th Inter. Conf. Eurohaptics 2002*, Edinburgh, July 2002, pp.6-11.

[53] Lord Corporation, *http://www.lord.com*

[54] E. P. Scilingo, N. Sgambelluri, D. De Rossi, A. Bicchi, "Towards a haptic Black Box for Free-hand Softness and Shape Exploration", *Proc. of the 2003 IEEE International Conference on Robotics & Automation*, Taipei, Taiwan, Sept. 14-19, 2003, pp. 2412-2417.

[55] A. Bicchi, M. Raugi, R. Rizzo, and N. Sgambelluri; "Analysis and Design of an Electromagnetic System for the Characterization of Magneto-Rheological Fluids for Haptic Interfaces", *IEEE Trans on Mag.*, Vol. 41, no. 5, pp. 1876-1879, May 2005.

[56] R. Rizzo, N. Sgambelluri, E. P. Scilingo, M. Raugi, and A. Bicchi; "Electromagnetic Modeling and Design of Haptic Interface Prototypes Based on Magnetorheological Fluids", *IEEE Trans on Mag.*, Vol. 43, Issue 9, Sept. 2007 pp. 3586 - 3598.

[57] A. Musolino, B. Tellini, M. Raugi, "3D Field Analysis in Tubular Induction Launchers with Armature Transverse Motion", *IEEE Trans. Mag.*, vol. 35, p. 154-159, 1999.

[58] A. Musolino and R. Rizzo "Numerical modeling of helical launchers", *IEEE Transactions on Plasma Science*, vol. 39, pp. 935-940, 2011.

[59] A. Musolino and R. Rizzo, "Numerical analysis of brush commutation in helical coil electromagnetic launchers", *IET Science, Measurement and Technology*, vol. 5, n. 4, pp. 147-154, 2011.

[60] Ambrosi G., A. Bicchi, D. De Rossi, and P. Scilingo, "The Role of Contact Area Spread Rate in Haptic discrimination of Softness", *Proceedings of the 1999 IEEE international Conference on Robotics and Automation*, pp. 305-310, Detroit, Michigan, may 1999.

[61] MEGA, User Manual, Bath University, Nov. 2000.

[62] EFFE v2.00, User Manual, Bathwick Electrical Design ltd, Jan. 2009.

[63] Coles, P.C.a , Rodger, D.a, Hill-Cottingham, R.J.a, Lai, H.C.a, Lamperth, M.b, Walker, A.b, "Design and analysis of an axial flux permanent magnet machine", *Second International Conference on Power Electronics, Machines and Drives, PEMD 2004*, vol. 2, pp. 840-843, 2004.

[64] A. Musolino, M. Raugi, B. Tellini, "Pulse Forming Network Optimal Design for the Power Supply of Eml Launchers". *IEEE Trans on Mag.*, vol. 33, no. 1, 1997.

[65] S. Barmada, et al, "Force and torque evaluation in hybrid FEM-MOM formulations", *IEEE Trans. Mag.*, Vol. 37, No. 5, 3108-3111, Sep. 2001.

[66] A. Musolino, "Finite-element method/method of moments Formulation for the Analysis of Current Distribution in Rail Launchers". *IEEE Trans. Mag.*, vol. 41, p. 387-392, 2005.

[67] N. Esposito, A. Musolino, M. Raugi, "Modelling of Three Dimentional Nonlinear Eddy Currents Problems with Conductors in Motion by an Integral Formulation", *IEEE Trans. Mag.*, vol. 32, no. 3, pp. 764-767, 1996.

[68] A. Musolino, "Numerical Analysis of a Rail Launcher with a Multilayered Armature", *IEEE Transactions on Plasma Science*, vol. 39, p. 788-793, 2011.

[69] S. Barmada, A. Musolino, M. Raugi, R. Rizzo, "Numerical Simulation of a Complete Generator-Rail Launch System", *IEEE Trans. Mag.*, vol. 41, pp. 369-374, 2005.

[70] N. Sgambelluri, E. P. Scilingo, A. Bicchi, R. Rizzo, M. Raugi; "Advanced modelling and preliminary psychophysical experiments for a free-hand haptic device", In *Proc. IEEE/RSJ Int. Conf. on Intelligent Robots and Systems 2006*, pp. 1558 - 1563, 2006.